

Magnetic and magnetocaloric properties of the amorphous Tb₃₁Co₆₉ and Dy₃₁Co₆₉ thin films deposited on Si substrates

P. Skokowski^{a,*}, M. Matczak^a, Ł. Frąckowiak^a, T. Bednarchuk^b, M. Kowacz^a, B. Anastaziak^{a,c}, K. Synoradzki^a

^a*Institute of Molecular Physics, Polish Academy of Sciences, Smoluchowskiego 17, 60-179 Poznań, Poland*

^b*Institute of Low Temperatures and Structural Research, Polish Academy of Sciences, Okólna 2, 50-422 Wrocław, Poland*

^c*NanoBioMedical Centre, Adam Mickiewicz University, Wszechnicy Piastowskiej 3, 61-614 Poznań, Poland*

Abstract

We present the structural, magnetic, and magnetocaloric properties of amorphous thin films Tb-Co and Dy-Co with stoichiometry Tb₃₁Co₆₉ and Dy₃₁Co₆₉, deposited on naturally oxidized silicon Si (100) substrates. Samples with a thickness $d = 50$ nm covered with a protective Au overlayer with a thickness $d_{\text{Au}} = 5$ nm were produced using the pulsed laser deposition technique. The X-ray diffraction analysis indicated the presence of a crystallized Laves phase in the prepared materials. Magnetization measurements as a function of temperature revealed ferrimagnetic behavior in both samples. We estimated the compensation temperature T_{comp} of the amorphous phase for Tb₃₁Co₆₉ at 81.5 K and for Dy₃₁Co₆₉ at 88.5 K, while we found the Curie temperature $T_{\text{C, Laves}}$ of the crystallized Laves phases at 204.5 K and at 117 K, respectively. We investigated the magnetocaloric effect in a wide temperature range, covering T_{comp} of amorphous phases and $T_{\text{C, Laves}}$ of crystallized Laves phases. The analysis for the magnetic field change of $\Delta\mu_0 H = 5$ T showed values of the magnetic entropy change of $-\Delta S_{\text{M}} = 4.9 \text{ mJ cm}^{-3} \text{ K}^{-1}$ at T_{comp} and $-\Delta S_{\text{M}} = 6.6 \text{ mJ cm}^{-3} \text{ K}^{-1}$ at $T_{\text{C, Laves}}$ for Tb₃₁Co₆₉, while for Dy₃₁Co₆₉, we determined the values of $-\Delta S_{\text{M}} = 35 \text{ mJ cm}^{-3} \text{ K}^{-1}$ at T_{comp} and $-\Delta S_{\text{M}} = 28 \text{ mJ cm}^{-3} \text{ K}^{-1}$ at $T_{\text{C, Laves}}$.

Keywords: thin films, amorphous rare-earth films, magnetocaloric effect

1. Introduction

Scientific investigation of materials involving rare-earth elements provided an opportunity to discover numerous physical phenomena, such as the Kondo effect, the heavy fermion state, unconventional superconductivity, or topological phases [1–3]. The realization of thin films of rare-earth alloys or multilayers utilizes the ferrimagnetic properties of the prepared materials. One of the widely studied systems is Tb-Co, which may find application by involving all-optical switching, movement of domain walls, current-induced magnetization switching, or the creation of skyrmions [4–7]. Dy-Co systems have been studied in the context of magnetic memories in DyCo₅ or also skyrmions creation in DyCo₃ thin films [8–10]. The search for new applications for thin films containing rare-earth elements is especially promising for systems where various physical phenomena occur.

The amorphous Tb-Co and Dy-Co systems in the form of thin layers exhibit a wide range of magnetic properties depending on the stoichiometry of the layers. Both systems are characterized as ferrimagnets [11, 12]. For Tb_{1-x}Co_x, the Curie temperature T_{C} is below 200 K for

Co concentration $x < 0.6$ and increases rapidly for the Co amount of $x > 0.6$ [12]. In the Dy_xCo_{100-x} system, the evolution of the compensation temperature T_{comp} is visible in the Dy concentration range, reaching room temperature for $x = 25$ [11]. On the other hand, hydrogen-amorphized TbCo₂H_{3.1} and DyCo₂H_{3.1} presents similar compensation temperature with $T_{\text{comp}} = 98.2$ and $T_{\text{comp}} = 93.0$, respectively, indicating weak R-Co interactions [13].

Magnetic materials containing rare-earth elements have been widely studied for magnetocaloric applications. Although multiple promising bulk materials have been discovered, other forms of materials are being investigated. Most known magnetocaloric materials, such as Gd, Gd₅(Si, Ge)₄, amorphous GdFeCo, or perovskites, have been verified in the form of thin films [14–19]. The results indicate that further studies may improve the magnetocaloric properties of some materials.

In this article, we present magnetic and magnetocaloric studies of the amorphous thin films Tb-Co and Dy-Co with stoichiometry Tb₃₁Co₆₉ and Dy₃₁Co₆₉ deposited using the pulsed laser deposition (PLD) technique. The thickness of the thin films studied was $d = 50$ nm for both materials. The films were prepared on naturally oxidized silicon Si (100) substrates. The X-ray diffraction (XRD) measurements revealed the presence of crystallized RCo₂ Laves phases. The magnetic properties of samples were investigated in the form of magnetization measurements

*Corresponding author

Email address: przemyslaw.skokowski@ifmpan.poznan.pl (P. Skokowski)

as a function of temperature and magnetic field. For both samples, the analysis of the first derivative revealed compensation temperatures T_{comp} below 100 K of the amorphous phase and Curie temperatures $T_{\text{C, Laves}}$ of the crystallized $R\text{Co}_2$ Laves phases. As the magnetocaloric effect of the TbCo_2 and DyCo_2 Laves phase presents good magnetocaloric parameters, the samples were studied in a wide range of temperatures to cover T_{comp} of the amorphous phases and also $T_{\text{C, Laves}}$ of the corresponding bulk compounds [20]. On this basis, the magnetocaloric parameters were determined: magnetic entropy change ΔS_{M} and temperature-averaged entropy change (TEC).

2. Experimental

The layers were deposited from commercially produced targets (Kurt Lesker) with a nominal stoichiometry of 1:2 of Tb and Dy to Co using the PLD technique (Nd:YAG laser). The laser wavelength was $\lambda = 532$ nm with a frequency of 2 Hz. The chamber pressure was about 8×10^{-8} mbar. Thin films were deposited on naturally oxidized Si (100) substrates. The nominal thickness of the Tb-Co and Dy-Co layers was $d = 50$ nm. The layers were covered with an Au layer $d_{\text{Au}} = 5$ nm deposited using the same PLD parameters to protect against oxidation.

The stoichiometry of the prepared samples and their topography were studied by scanning electron microscopy (SEM) and energy dispersive spectroscopy (EDS). The device used for this purpose was a FEI Nova NanoSEM 650 equipped with an EDS Bruker detector.

The crystal structure of the prepared samples was examined by XRD measurements at room temperature using the X'pert Pro PANalytical device with a Cu $K\alpha$ radiation source.

Magnetic properties investigation was performed on the Quantum Design Physical Property Measurement System (QD PPMS) in DC magnetization mode using a vibrating sample magnetometer (VSM). Measurements of magnetization were collected as a function of temperature in zero-field cooling (ZFC) and field cooling (FC) modes. The experiments were carried out in the temperature range of 10-380 K with a magnetic field of 0.1 T. The isothermal magnetization was measured as a function of the applied magnetic field at magnetic field values up to 5 T in various temperature ranges.

3. Results

3.1. Microstructure investigation

The first step was the verification of the chemical composition of the samples using EDS. The atomic percentage results showed that the stoichiometry of all samples was close to the nominal stoichiometry. For the Tb-Co layer, the atomic percentage content was 30.8(1.4)% of Tb and 69.2(1.4)% of Co, while for the Dy-Co layer, it was 30.9(0.7)% of Dy and 69.1(0.7)% of Co. The nominal

atomic percentage content is expected to be 33% of Tb or Dy and 67% of Co. Due to the stoichiometry, the samples are labeled $\text{Tb}_{31}\text{Co}_{69}$ and $\text{Dy}_{31}\text{Co}_{69}$. For both samples, the SEM images (not shown) presented material droplets on the surface of the layers, which is characteristic of the PLD method. Chemical maps (not shown) indicated the uniform distribution of all elements on the sample surface.

3.2. X-ray diffraction

The XRD results for the samples with the $\text{Tb}_{31}\text{Co}_{69}$ and $\text{Dy}_{31}\text{Co}_{69}$ layers are shown in Figure 1(a) and (b). The results for the entire 2θ range for both samples (not shown) revealed two major maxima, one at $2\theta = 69.3^\circ$, which is related to the Si (400) peak, and the other allocated at $2\theta = 38.3^\circ$, which is related to the Au (111) peak. For both samples, in the vicinity of the Au (111) peak, small peaks are observed around $2\theta = 33.1^\circ$. These reflections were assigned to a close approximation of the position of the (220) peak of the MgCu_2 -type structure of TbCo_2 and DyCo_2 Laves phases [21, 22]. The peak position is comparable for both compounds, suggesting that the values of the lattice parameters a are very similar, although slight differences in the crystal lattice parameters of bulk TbCo_2 and DyCo_2 were observed [21, 22]. Although the presence of Laves phases is noted, the low intensities of the peaks of the (220) peaks suggest that the crystallized volume of the amorphous R -Co layers is small. The schematic composition of the samples is presented in Figure 1(c).

3.3. Magnetic properties

Magnetization as a function of temperature is presented in Figure 2(a) and (b) for samples with $\text{Tb}_{31}\text{Co}_{69}$ and $\text{Dy}_{31}\text{Co}_{69}$ layers. The ZFC and FC curves show no distinct magnetic phase transitions for both samples. The main visible feature of the results obtained is a bifurcation of these curves, observed at 200 K for the sample with the $\text{Tb}_{31}\text{Co}_{69}$ layer and at 120 K for the sample with the $\text{Dy}_{31}\text{Co}_{69}$ layer. The first derivative was used to verify the presence of phase transitions. Several local extrema are registered for both samples. The first local extrema are detectable in the temperature range of 100 K for both layers. This observation is in good approximation with the results for the amorphous $R\text{Co}_2$ obtained in the hydrogenation process, with $T_{\text{comp}} = 98$ K for the TbCo_2 stoichiometry and $T_{\text{comp}} = 93$ K for the DyCo_2 stoichiometry [13]. The second local extrema are observed around 230 K and 130 K for the samples with $\text{Tb}_{31}\text{Co}_{69}$ and $\text{Dy}_{31}\text{Co}_{69}$ layers, respectively. These temperatures correspond to $T_{\text{C, Laves}}$ of the TbCo_2 ($T_{\text{C, bulk}} = 230$ K) and DyCo_2 ($T_{\text{C, bulk}} = 135$ K) Laves phases. However, in the ZFC and FC curves, the transitions are barely visible as an inflection point, which confirms the minimal contribution of the crystallized Laves phases. Furthermore, for the sample with the $\text{Tb}_{31}\text{Co}_{69}$ layer, a local maximum of the derivative around 350 K was registered. The maximum is related to $T_{\text{C, amorph}}$ of the amorphous phase [12].

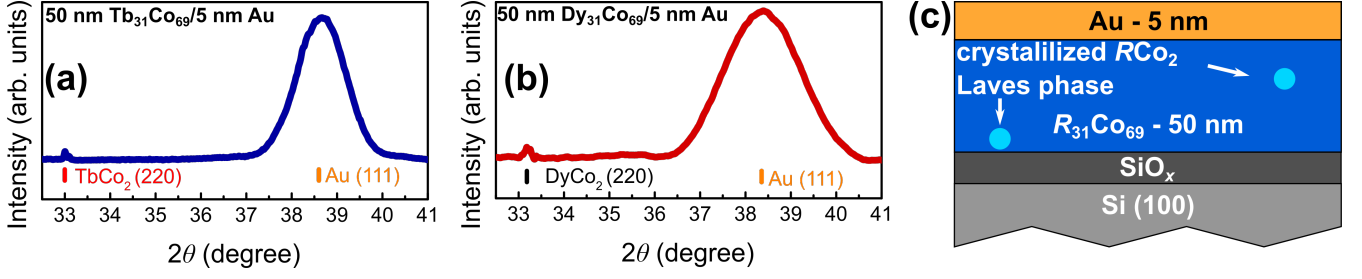


Figure 1: (a) and (b) X-ray diffraction patterns of the TbCo₂ and DyCo₂ layers. Wide maxima at $2\theta = 38.3^\circ$ are related to the Au (111) peak, small maxima at $2\theta = 33.1^\circ$ are related to the TbCo₂ and DyCo₂ (220) peaks. (c) Schematic illustration of the samples studied. Small light blue balls indicate crystals of the $R\text{Co}_2$ Laves phase.

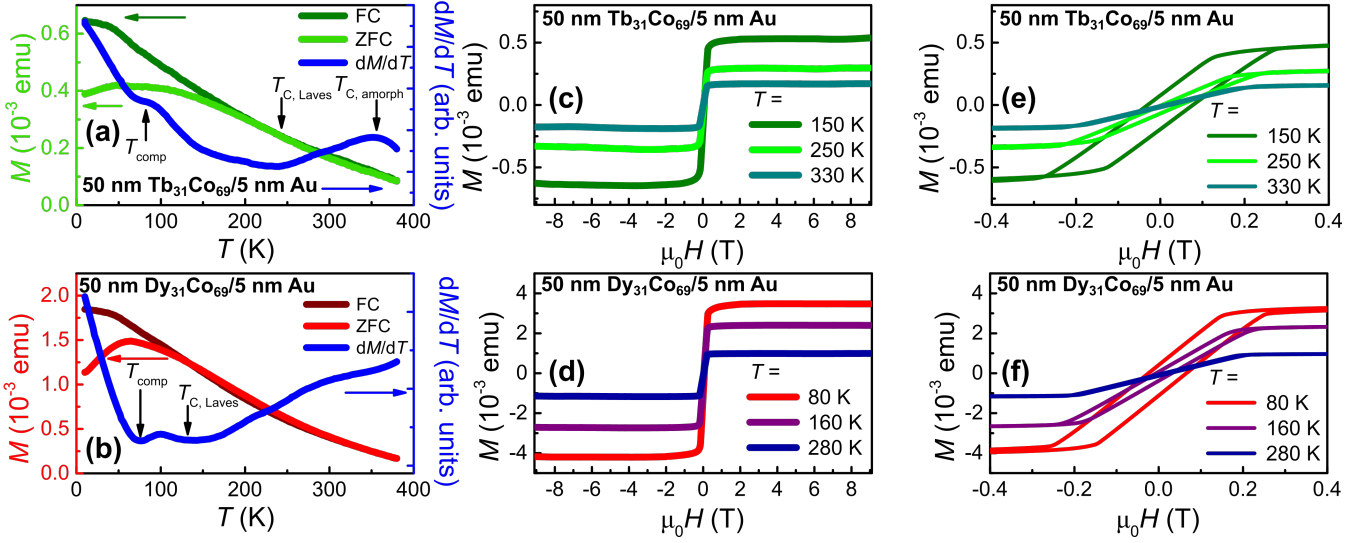


Figure 2: Magnetic properties of the samples with the Tb₃₁Co₆₉ and Dy₃₁Co₆₉ layers. (a) and (b) Magnetization as a function of temperature measured in a magnetic field value of 0.1 T for the Tb₃₁Co₆₉ and Dy₃₁Co₆₉ layers. The right blue axis is assigned to the derivative of the FC magnetization. The amorphous phase compensation temperatures are denoted as T_{comp} . The Curie temperatures of crystallized Laves phases are denoted as $T_{\text{C, Laves}}$. For Tb₃₁Co₆₉ at around 350 K $T_{\text{C, amorph}}$ of the amorphous phase is noted. (c) and (d) Magnetization isotherms as a function of an applied magnetic field for the Tb₃₁Co₆₉ and Dy₃₁Co₆₉ layers. (e) and (f) Close up on the hysteresis of the magnetization isotherms as a function of an applied magnetic field for the Tb₃₁Co₆₉ and Dy₃₁Co₆₉ layers.

Magnetization as a function of the magnetic field was examined at different temperatures for both samples. The results are presented in Figures 2(c) and (d). The magnetization curves show ferrimagnetic behavior for all tested temperatures for both layers. The magnetization values increase with decreasing temperature. The close-up of the hysteresis is shown in Figures 2(e) and (f). In both cases, the hysteresis is not noticeable at the highest measured temperatures. The hysteresis increases with decreasing temperatures with coercivity up to 0.1 T at 150 K for the Tb₃₁Co₆₉ layer and up to 0.09 T at 80 K for the Dy₃₁Co₆₉ layer.

3.4. Magnetocaloric properties

The magnetocaloric effect was determined for the samples studied in the temperature range, which includes T_{comp} of the amorphous majority of the samples and $T_{\text{C, Laves}}$ of the small contribution of the Laves phases. The first quarters of the magnetization isotherms as a func-

tion of the magnetic field collected at exemplary temperatures for samples with Tb₃₁Co₆₉ and Dy₃₁Co₆₉ layers are presented in Figure 3(a) and (b). Figure 3(c) and (d) show Arrott plots in the form of M^2 as a function of $\mu_0 H/M$. The samples do not exhibit negative curvature, indicating the second-order type phase transition [23]. For bulk TbCo₂ and DyCo₂ Laves phases, the first-order type phase transition is expected [24–27].

After collecting the experimental results of the magnetization isothermal measurements, the magnetic entropy change ΔS_M could be calculated according to the formula [28]:

$$\Delta S_M \approx \frac{\mu_0}{\Delta T} \left[\int_0^{H_{\text{max}}} M(T + \Delta T, H) dH - \int_0^{H_{\text{max}}} M(T, H) dH \right], \quad (1)$$

where: μ_0 – the magnetic permeability of the vacuum, H_{max} – the maximum magnetic field value to calculate the

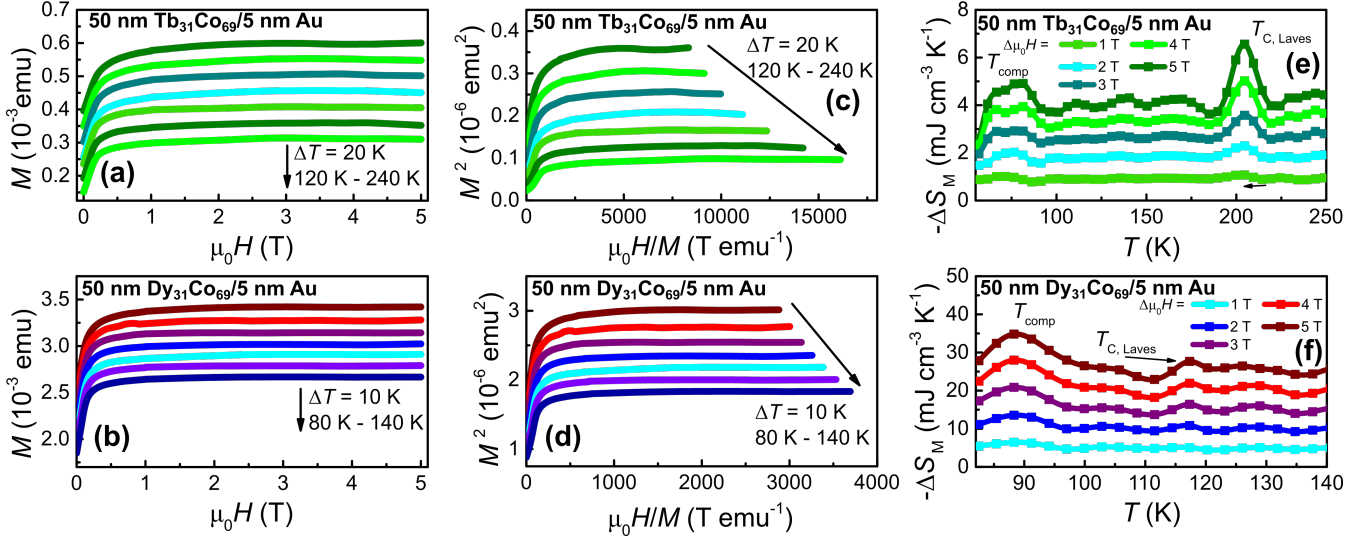


Figure 3: (a) and (b) Magnetization isotherms as a function of magnetic field measured at exemplary temperatures for the samples with $\text{Tb}_{31}\text{Co}_{69}$ and $\text{Dy}_{31}\text{Co}_{69}$ layers. (c) and (d) Arrott plots for the samples with $\text{Tb}_{31}\text{Co}_{69}$ and $\text{Dy}_{31}\text{Co}_{69}$ layers. (e) and (f) Magnetic entropy change ΔS_M for the $\text{Tb}_{31}\text{Co}_{69}$ and $\text{Dy}_{31}\text{Co}_{69}$ layers for various magnetic field values.

specific $\Delta S_M(T, H_{\text{max}})$, ΔT – the temperature difference between two closest magnetization isotherms, $M(T, H)$ – magnetization for the specific magnetic field value and temperature T , $M(T + \Delta T, H)$ – magnetization for specific magnetic field value and temperature $T + \Delta T$. To describe how the ΔS_M peak spans over a temperature range, the temperature-averaged entropy change TEC was calculated for lift temperatures of $\Delta T_{\text{lift}} = 3$ K and 10 K. The value of this parameter is calculated using the following formula [29]:

$$TEC(\Delta T_{\text{lift}}) = \frac{1}{\Delta T_{\text{lift}}} \max_{T_{\text{mid}}} \left\{ \int_{T_{\text{mid}} - \frac{\Delta T_{\text{lift}}}{2}}^{T_{\text{mid}} + \frac{\Delta T_{\text{lift}}}{2}} \Delta S_M(T) \mu_0 H dT \right\}, \quad (2)$$

where: ΔT_{lift} – the desired lift temperature, T_{mid} – the temperature of the center of the TEC calculated to maximize the TEC value. Another magnetocaloric parameter, the relative cooling power RCP , was not determined because, in the samples studied, the full width at half the maxima of the peaks could not be found in the measured temperature range.

In order to evaluate the ΔS_M values in $\text{mJ cm}^{-3} \text{K}^{-1}$ units for the deposited R -Co layers, it was necessary to determine the volume of the layers. The volume of the deposited layers was assumed to be the area of the samples multiplied by the thickness of the layers. The ΔS_M results obtained for the deposited R -Co layers are shown in Figures 3(e) and (f), while the values of all magnetocaloric parameters are gathered in Table 1. For both samples, two maxima connected to the amorphous T_{comp} and to the $T_{\text{C, Laves}}$ of the Laves phases are observed. In the case of the $\text{Tb}_{31}\text{Co}_{69}$ sample, the TbCo_2 Laves phase-related

peak is more pronounced and is at 204.5 K, shifted towards lower temperatures compared to the bulk crystallized TbCo_2 sample. The amorphous T_{comp} -related maximum is at 81.5 K. The maximum values for both maxima are very low, below $7 \text{ mJ cm}^{-3} \text{K}^{-1}$ for the magnetic field change of $\mu_0 H = 5$ T, see Table 1. The width of the ΔS_M maxima described by TEC indicates that for both peaks, the ΔS_M values do not change significantly, even for $TEC(10)$. For the $\text{Dy}_{31}\text{Co}_{69}$ layer, the ΔS_M maximum related to the amorphous T_{comp} is at a temperature 88.5 K, and another less pronounced maximum is probably related to the DyCo_2 Laves phase at 117 K. The values of the obtained ΔS_M at T_{comp} is $35 \text{ mJ cm}^{-3} \text{K}^{-1}$, while at $T_{\text{C, Laves}}$ of the Laves phase is $28 \text{ mJ cm}^{-3} \text{K}^{-1}$. $TEC(3)$ and $TEC(10)$ values for this sample also indicate small changes of ΔS_M over the specific temperature range.

It is important to note that both samples are in a ferrimagnetic state in the temperature range studied, since the $T_{\text{C, amorph}}$ of the amorphous RCO_2 alloys is over 300 K [11, 12]. Therefore, the values of magnetocaloric parameters are relatively low. However, the contribution to ΔS_M of T_{comp} is noticeable even in the ferrimagnetic state. While for the sample with $\text{Dy}_{31}\text{Co}_{69}$ layer, ΔS_M has higher values at T_{comp} , for the sample with $\text{Tb}_{31}\text{Co}_{69}$ layer, ΔS_M at $T_{\text{C, Laves}}$ of the crystallized Laves phase has higher values. Although the Laves phase contribution is observed, the content of this phase in the sample volume is low, resulting in a low contribution to the ΔS_M values.

4. Summary

The thin films of the amorphous Tb-Co and Dy-Co were prepared and deposited on a naturally oxidized Si (100) substrate. The thickness of the layers was $d = 50$ nm covered with an Au overlayer with a thickness of

Table 1: Maximum value of magnetic entropy change ΔS_M^{\max} , temperature of maximum ΔS_M^{\max} value T_{max} and temperature averaged entropy change $TEC(3)$ and $TEC(10)$ for the $Tb_{31}Co_{69}$ and $Dy_{31}Co_{69}$ layers. The parameter values were obtained for the magnetic field change of $\Delta\mu_0 H = 5$ T. For both samples the determined values refer to maxima related to the T_{comp} of amorphous phase and to the $T_{C, Laves}$ of the crystallized Laves phase.

Parameters	$Tb_{31}Co_{69}$, T_{comp}	$Tb_{31}Co_{69}$, $T_{C, Laves}$	$Dy_{31}Co_{69}$, T_{comp}	$Dy_{31}Co_{69}$, $T_{C, Laves}$
ΔS_M^{\max} (mJ cm ⁻³ K ⁻¹)	4.9	6.6	35	28
T_{max} (K)	81.5	204.5	88.5	117
$TEC(3)$ (mJ cm ⁻³ K ⁻¹)	4.8	6.4	34	27
$TEC(10)$ (mJ cm ⁻³ K ⁻¹)	4.7	6.2	33	26

$d_{Au} = 5$ nm. Scanning electron microscopy and energy dispersive spectroscopy showed a homogeneous chemical distribution with atomic stoichiometry of $Tb_{31}Co_{69}$ and $Dy_{31}Co_{69}$. The presence of crystallized Laves phases in the layers was verified by X-ray diffraction, which revealed low intensity maxima associated with the (220) peak for both thin films. Analysis of the magnetization results as a function of temperature for both samples revealed the compensation temperature of the amorphous phases and the Curie temperature of the corresponding Laves phase compounds. The magnetization as a function of the magnetic field indicated ferrimagnetism for both samples at all measured temperatures.

The magnetocaloric effect was investigated in a wide temperature range. The obtained results of the magnetic entropy change ΔS_M revealed maxima connected with the compensation temperature T_{comp} of the amorphous phase and with phase transitions connected with the presence of crystallized Laves phases. These contributions to the ΔS_M are visible in the ferrimagnetic state of $Tb_{31}Co_{69}$ and $Dy_{31}Co_{69}$ layers.

Acknowledgments

PS acknowledges the financial support of the National Science Centre Poland under the decision 2021/05/X/ST5/ 00763. The authors would like to thank Piotr Kuświk from the Department of Thin Films and Nanostructures IMP PAS for the discussion and helpful comments.

References

- [1] D. Li, K. Lee, B. Y. Wang, M. Osada, S. Crossley, H. R. Lee, Y. Cui, Y. Hikita, H. Y. Hwang, Superconductivity in an infinite-layer nickelate, *Nature* 572 (2019) 624–627.
- [2] M. Smidman, O. Stockert, E. M. Nica, Y. Liu, H. Yuan, Q. Si, F. Steglich, Colloquium: Unconventional fully gapped superconductivity in the heavy-fermion metal $CeCu_2Si_2$, *Rev. Mod. Phys.* 95 (2023) 031002.
- [3] X. Xu, J.-X. Yin, Z. Qu, S. Jia, Quantum interactions in topological r166 kagome magnet, *Rep. Prog. Phys.* 86 (2023) 114502.
- [4] L. Caretta, M. Mann, F. Büttner, K. Ueda, B. Pfau, C. M. Günther, P. Hessler, A. Churikova, C. Klose, M. Schneider, et al., Fast current-driven domain walls and small skyrmions in a compensated ferrimagnet, *Nat. Nanotechnol.* 13 (2018) 1154–1160.
- [5] Ł. Frąckowiak, P. Kuświk, G. D. Chaves-O’Flynn, M. Urbaniak, M. Matczak, P. P. Michałowski, A. Maziewski, M. Reginka, A. Ehresmann, F. Stobiecki, Magnetic domains without domain walls: A unique effect of He⁺ ion bombardment in ferrimagnetic Tb/Co films, *Phys. Rev. Lett.* 124 (2020) 047203.
- [6] L. Avilés-Félix, A. Olivier, G. Li, C. S. Davies, L. Álvaro-Gómez, M. Rubio-Roy, S. Auffret, A. Kirilyuk, A. Kimel, T. Rasing, et al., Single-shot all-optical switching of magnetization in Tb/Co multilayer-based electrodes, *Sci. Rep.* 10 (2020) 5211.
- [7] Y. Guo, Y. Wu, Y. Cao, X. Zeng, B. Wang, D. Yang, X. Fan, J. Cao, The deterministic field-free magnetization switching of perpendicular ferrimagnetic Tb-Co alloy film induced by interfacial spin current, *Appl. Phys. Lett.* 119.
- [8] A. Ünal, S. Valencia, F. Radu, D. Marchenko, K. Merazzo, M. Vázquez, J. Sánchez-Barriga, Ferrimagnetic DyCo₅ nanostructures for bits in heat-assisted magnetic recording, *Phys. Rev. Appl.* 5 (2016) 064007.
- [9] K. Chen, D. Lott, A. Philippi-Kobs, M. Weigand, C. Luo, F. Radu, Observation of compact ferrimagnetic skyrmions in DyCo₃ film, *Nanoscale* 12 (2020) 18137–18143.
- [10] C. Luo, K. Chen, V. Ukleev, S. Wintz, M. Weigand, R.-M. Abrudan, K. Prokeš, F. Radu, Direct observation of Néel-type skyrmions and domain walls in a ferrimagnetic DyCo₃ thin film, *Commun. Phys.* 6 (2023) 218.
- [11] M. Takahashi, T. Shimamori, T. Miyazaki, T. Wakiyama, A. Yoshihara, Perpendicular magnetic anisotropy and magnetostriction of evaporated Co-(Pr, Nd, Gd, Dy, Er) amorphous binary alloy films, *IEEE Transl. J. Magn. Jpn.* 4 (1989) 666–672.
- [12] M. Soltani, N. Chakri, M. Lahoubi, Composition and annealing dependence of magnetic properties in amorphous Tb–Co based alloys, *J. Alloy. Compd.* 323 (2001) 422–426.
- [13] N. Mushnikov, V. Gaviko, T. Goto, Magnetic properties of hydrogen-amorphized RCO_2H_x ($R = Gd, Tb, Dy, Ho, Er, Tm$ and Y) alloys, *J. Alloy. Compd.* 398 (2005) 36–41.
- [14] H. F. Kirby, D. D. Belyea, J. T. Willman, C. W. Miller, Effects of preparation conditions on the magnetocaloric properties of Gd thin films, *J. Vac. Sci. Technol. A* 31.
- [15] C. W. Miller, D. D. Belyea, B. J. Kirby, Magnetocaloric effect in nanoscale thin films and heterostructures, *J. Vac. Sci. Technol. A* 32.
- [16] R. L. Hadimani, J. H. Silva, A. M. Pereira, D. L. Schlagel, T. A. Lograsso, Y. Ren, X. Zhang, D. C. Jiles, J. P. Araújo, Gd₅(Si, Ge)₄ thin film displaying large magnetocaloric and strain effects due to magnetostructural transition, *Appl. Phys. Lett.* 106.
- [17] D. Matte, M. De Lafontaine, A. Ouellet, M. Balli, P. Fournier, Tailoring the magnetocaloric effect in La₂NiMnO₆ thin films, *Phys. Rev. Appl.* 9 (2018) 054042.
- [18] H. Bouhani, A. Endicchi, D. Kumar, O. Copie, H. Zaari, A. David, M. Fouchet, W. Prellier, O. Mounkachi, M. Balli, et al., Engineering the magnetocaloric properties of PrVO₃ epitaxial oxide thin films by strain effects, *Appl. Phys. Lett.* 117.
- [19] G. J. Kumar, Z. Guo, L. Gu, J. Feng, K. Kamala Bharathi, K. Wang, Broad table-like magnetocaloric effect in GdFeCo

- thin-films for room temperature Ericsson-cycle magnetic refrigeration, *J. Appl. Phys.* 135.
- [20] N. K. Singh, K. Suresh, A. Nigam, S. Malik, A. Coelho, S. Gama, Itinerant electron metamagnetism and magnetocaloric effect in $R\text{Co}_2$ -based Laves phase compounds, *J. Magn. Magn. Mater.* 317 (2007) 68–79.
 - [21] S. Khmelevskiy, P. Mohn, The order of the magnetic phase transitions in $R\text{Co}_2$ (R = Rare Earth) intermetallic compounds, *J. Phys.: Condens. Mat.* 12 (2000) 9453.
 - [22] T. Chang, C. Zhou, J. Mi, K. Chen, F. Tian, Y.-S. Chen, S. G. Wang, Y. Ren, D. E. Brown, X. Song, et al., Crystal structures and phase relationships in magnetostrictive $\text{Tb}_{1-x}\text{Dy}_x\text{Co}_2$ system, *J. Phys.: Condens. Mat.* 32 (2019) 135802.
 - [23] A. Arrott, Criterion for ferromagnetism from observations of magnetic isotherms, *Phys. Rev.* 108 (1957) 1394.
 - [24] D. Huang, J. Gao, S. H. Lapidus, D. E. Brown, Y. Ren, Exotic hysteresis of ferrimagnetic transition in Laves compound TbCo_2 , *Mater. Res. Lett.* 8 (2020) 97–102.
 - [25] B. Ahuja, H. Mund, J. Sahariya, A. Dashora, M. Halder, S. Yusuf, M. Itou, Y. Sakurai, Temperature dependent spin and orbital magnetization in TbCo_2 : Magnetic Compton scattering and first-principles investigations, *J. Alloy. Compd.* 633 (2015) 430–434.
 - [26] C. Zhou, T. Chang, Z. Dai, Y. Chen, C. Guo, Y. Matsushita, X. Ke, A. Murtaza, Y. Zhang, F. Tian, et al., Unified understanding of the first-order nature of the transition in TbCo_2 , *Phys. Rev. B* 106 (2022) 064409.
 - [27] K. Morrison, A. Dupas, Y. Mudryk, V. Pecharsky, K. Gschneidner, A. Caplin, L. Cohen, Identifying the critical point of the weakly first-order itinerant magnet DyCo_2 with complementary magnetization and calorimetric measurements, *Phys. Rev. B* 87 (2013) 134421.
 - [28] K. A. Gschneidner, V. Pecharsky, A. Tsokol, Recent developments in magnetocaloric materials, *Rep. Prog. Phys.* 68 (2005) 1479.
 - [29] L. Griffith, Y. Mudryk, J. Slaughter, V. Pecharsky, Material-based figure of merit for caloric materials, *J. Appl. Phys.* 123 (2018) 034902.